Thomas–Fermi–von Weizsäcker theory for a harmonically trapped, two-dimensional, spin-polarized dipolar Fermi gas

B. P. van Zyl
Department of Physics, St. Francis Xavier University, Antigonish, Nova Scotia, Canada B2G 2W5

E. Zaremba and P. Pisarski
Department of Physics, Astronomy and Engineering Physics, Queen's University, Kingston, Ontario, Canada K7L 3N6

(Received 30 November 2012; published 10 April 2013)

We systematically develop a density functional description for the equilibrium properties of a two-dimensional, harmonically trapped, spin-polarized dipolar Fermi gas based on the Thomas–Fermi–von Weizsäcker approximation. We pay particular attention to the construction of the two-dimensional kinetic energy functional, where corrections beyond the local density approximation must be motivated with care. We also present an intuitive derivation of the interaction energy functional associated with the dipolar interactions and provide physical insight into why it can be represented as a local functional. Finally, a simple and highly efficient self-consistent numerical procedure is developed to determine the equilibrium density of the system for a range of dipole interaction strengths.

DOI: 10.1103/PhysRevA.87.043614 PACS number(s): 03.75.Ss, 31.15.E−, 71.10.Ca, 05.30.Fk

I. INTRODUCTION

Ultracold, trapped dipolar quantum gases have received increasing attention over the past decade owing to the inherently interesting properties of the anisotropic and long-range nature of the dipole-dipole interaction [1]. One of the important consequences of the anisotropy is that the interactions between the particles can be tuned from being predominantly attractive to repulsive by simply changing the three-dimensional (3D) trapping geometry or, for dipoles confined to the 2D x-y plane, by adjusting the orientation of the dipoles relative to the z axis [1,2]. Therefore, novel physics in both the equilibrium and dynamic properties of such systems may be explored as a function of the strength of the interaction, the geometry of the confining potential, and the dimensionality of the system.

While the degenerate dipolar Bose gas has been well studied experimentally and theoretically [1], realizing a degenerate dipolar Fermi gas in the laboratory has proven to be much more elusive. One of the reasons for this is that the path to quantum degeneracy is impeded by the Pauli principle, which forbids s-wave collisions between identical atoms. Thus, early attempts to cool both magnetic and molecular dipolar Fermi gases below degeneracy were unsuccessful [3–6]. However, in the recent work of Lu *et al.* [7], this experimental hurdle was finally overcome, resulting in the experimental realization of a spin-polarized, degenerate dipolar Fermi gas. Specifically, using the method of sympathetic cooling, a mixture consisting of ^{161}Dy and the bosonic isotope ^{162}Dy was cooled to $T/T_F \sim 0.2$. In addition, this group was also able to evaporatively cool a single-component gas of ^{161}Dy down to a temperature of $T/T_F \sim 0.7$. This latter result is presumed to arise from the rethermalization provided by the strong dipolar scattering between the ^{161}Dy atoms which have a large magnetic moment ($\mu \sim 10\mu_B$).

The ability to fabricate such systems in the laboratory now opens the door for the investigation of both the equilibrium and dynamical properties of dipolar Fermi gases and will enable contact to be made with the large body of theoretical work already in the literature [1]. Moreover, it is now reasonable to expect that quasi-2D degenerate dipolar Fermi gases will also be realized experimentally, thereby allowing for studies into the stability, pairing, and superfluidity of low-dimensional dipolar systems, which to date have only been investigated theoretically [2,8,9].

With a view towards ultimately calculating the collective mode frequencies, we develop in this paper a density-functional theory (DFT) for the equilibrium properties of a degenerate, harmonically trapped, spin-polarized dipolar Fermi gas. Our theoretical framework is based on the Thomas–Fermi–von Weizsäcker (TFvW) approximation, which was previously formulated in the context of degenerate electron gases [10]. The mathematical framework of the TFvW theory is very simple, numerically easy to implement, and computationally inexpensive. The TFvW theory has also been shown to provide an exceedingly accurate description of equilibrium properties, as well as collective excitations (i.e., magnetoplasmons), of electronic systems in a variety of 2D and 3D confinement geometries [10–16]. Our purpose here is to take advantage of this approach, which is largely unknown in the cold-atom community, and apply it to the dipolar Fermi gas. We only address the equilibrium properties in this paper and leave the presentation of the more involved mode calculation to a future presentation. Moreover, in anticipation of forthcoming experiments, along with the goal of making contact with the recent theoretical work of Fang and Englert [17], we focus on the 2D geometry, although the extension of the theory to 3D is straightforward. The 2D geometry also allows for the development of exact analytical results, which we exploit to test the efficacy of the TFvW approximation.

The organization of our paper is as follows. In Sec. II, we construct the approximate kinetic energy functional for the trapped 2D system and show that it is necessary to go beyond the local-density approximation (LDA) in order to provide a more accurate determination of the ground-state energy, along with physically reasonable density profiles, for

the system. In Sec. III, we present an intuitive approach for the development of the interaction energy functional, in addition to providing physical insight into why the functional may be represented solely in terms of the *local* density. Section IV presents the details of the numerical procedure for implementing the TFvW, in addition to representative illustrations of the spatial density profile of the dipolar gas as the dipole-dipole interaction strength is changed. Finally, in Sec. V, we present our conclusions and closing remarks.

II. KINETIC ENERGY FUNCTIONAL

In the Kohn-Sham (KS) DFT [18], the noninteracting kinetic energy is treated exactly by solving N single-particle Schrödinger-like equations, yielding the KS orbitals, from which the kinetic energy may be constructed. However, the KS DFT is not quite in keeping with the spirit of the Hohenberg-Kohn theorems, [19] which provide a mathematical justification for the solution to the many-body problem solely in terms of the density of the system (i.e., an orbital free formulation). Indeed, in its purest form, DFT has no need for the calculation of orbitals of any kind. However, an orbital free DFT requires the specification of a noninteracting kinetic energy density functional which is not known exactly. The purpose of this section is to provide an approximate, but accurate, kinetic energy density functional to be used in a DFT description of the ground-state properties of a 2D harmonically trapped dipolar Fermi gas.

The first level of approximation for the explicit construction of the kinetic energy density functional is the local-density approximation [20]. In this approach, the exact kinetic energy density for a *homogeneous* system is determined, after which the same expression is assumed to be true locally for the *inhomogeneous* system. The LDA is generally valid for systems that are only weakly inhomogeneous, but may be remarkably accurate even for strongly inhomogeneous systems [21,22]. In the case of a uniform 2D system, the noninteracting kinetic energy for a spin-polarized 2D Fermi gas is found to be

$$E_K^{\rm hom} = \sum_{\mathbf{k}} n_{\mathbf{k}} \frac{\hbar^2 k^2}{2m} = A \frac{\pi \hbar^2}{m} \bar{n}_{\rm 2D}^2. \tag{1}$$

Here $n_{\mathbf{k}} = \theta(k_F - k)$ is the zero-temperature Fermi occupation number, k_F is the 2D Fermi wave vector given by $k_F^2 = 4\pi \bar{n}_{2D}$, $\bar{n}_{\rm 2D}$ is the uniform number density, and A is the area of the system. Invoking the LDA, the 2D kinetic energy functional for an inhomogeneous system takes the form

$$E_K[n] = \int d\mathbf{r} \frac{\pi \hbar^2}{m} n(\mathbf{r})^2. \tag{2}$$

If to this we add the energy $E_P[n]$ of the particles interacting with an external potential $v_{\rm ext}(\mathbf{r})$, we obtain the Thomas-Fermi (TF) energy functional,

$$E_{TF}[n] = \int d\mathbf{r} \frac{\pi \hbar^2}{m} n(\mathbf{r})^2 + \int d\mathbf{r}\, v_{\rm ext}(\mathbf{r}) n(\mathbf{r}). \tag{3}$$

A variational minimization of this equation with respect to the density leads to the Euler-Lagrange equation

$$\frac{\delta E_{TF}[n]}{\delta n(\mathbf{r})} - \mu_{TF} = 0, \tag{4}$$

where the Lagrange multiplier μ_{TF} (TF chemical potential) serves to fix the total number of particles. Using Eq. (3), Eq. (4) leads to the the TF spatial density, given explicitly as

$$n_{TF}(\mathbf{r}) = \frac{m}{2\pi\hbar^2} \left[\mu_{TF} - v_{\rm ext}(\mathbf{r})\right]. \tag{5}$$

The density is seen to vanish on the surface defined by $v_{\rm ext}(\mathbf{r}) = \mu_{TF}$ and is taken to be zero for all positions where $v_{\rm ext}(\mathbf{r}) > \mu_{TF}$. This unphysical behavior of the density is, of course, a consequence of the local nature of the TF energy functional and is also present in other spatial dimensions [23].

One may try to remove the unphysical behavior of the TF density by improving upon the quality of the kinetic energy functional. One possibility is introducing gradient corrections which take into account inhomogeneities of the density. Corrections of this kind can be developed in several ways [12,19,23–31]. For example, one can consider a weakly inhomogeneous system in which the density deviates only slightly from some uniform value [19]. However, if this method is used in 2D, it is found that *all gradient corrections vanish* [27,32]. The implication of this is that one cannot formally justify the inclusion of gradient corrections in 2D on the basis of a systematic expansion about the homogenous limit. Other methods, such as the semiclassical Wigner-Kirkwood (WK) expansion [12,23], do yield gradient corrections in 2D which, however, make no contribution to the total kinetic energy for physically smooth densities [33]. These observations, of course, do not mean that the LDA is exact in 2D since the TF approximation certainly does not generate the exact density of an inhomogeneous system. It is thus clear that nonlocal corrections to the kinetic energy functional are necessary, and it is plausible that they may still take the form of gradient corrections [31], similar to what are found in 1D and 3D inhomogeneous systems [27].

To demonstrate the need for nonlocal corrections in 2D explicitly, it is useful to consider a 2D gas of noninteracting particles trapped within the harmonic confining potential $v_{\rm ext}(r) = m\omega_0 r^2/2$. It was shown by Brack and van Zyl [21] that the exact spatial density is given by

$$n_{\rm ex}(r) = \frac{1}{\pi} \sum_{n=0}^{M} (-1)^n (M - n + 1) L_n(2r^2) e^{-r^2}, \tag{6}$$

where $L_n(x)$ is a Laguerre polynomial [34] and all lengths are expressed in units of the harmonic oscillator length $a_{\rm ho} = \sqrt{\hbar/m\omega_0}$. The integer, M, counts the number of filled oscillator shells; i.e., the Fermi energy is given by $E_F = \hbar\omega_0(M+1)$. Integrating Eq. (6) over all space leads to the total number of particles in the system as a function of the shell index

$$N(M) = \tfrac{1}{2}(M+1)(M+2). \tag{7}$$

The exact total energy of this system is found to be

$$E_{\rm ex} = \frac{\hbar\omega_0}{3} N\sqrt{1+8N}. \tag{8}$$

By virtue of the equipartition of the kinetic and potential energies in a harmonic trap, the exact kinetic energy is given by

$$E_{\rm ex}^K = \frac{\hbar\omega_0}{6} N\sqrt{1+8N} = \frac{1}{2}\hbar\omega_0\left[\frac{2\sqrt{2}}{3}N^{3/2} + \frac{1}{12\sqrt{2}}N^{1/2} + O(N^{-1/2})\right], \quad (9)$$

where in going to the last line in Eq. (9) we have made use of the large-N behavior of the exact kinetic energy.

The remarkable result found in Ref. [21] is that the LDA kinetic energy functional, Eq. (2), integrates to the *exact* kinetic energy when the exact density is used as input. As mentioned above, this should not be misconstrued to mean that Eq. (2) is, in fact, the exact kinetic energy functional for the harmonically trapped system, i.e., that no corrections beyond the LDA are required. The exact spatial density $n_{\rm ex}$ is emphatically not the density which variationally minimizes the TF energy functional. This density is given by Eq. (5) and may be written as

$$n_{TF}(\mathbf{r}) = \frac{1}{4\pi a_{\rm ho}^4}\left(R_{TF}^2 - r^2\right), \quad (10)$$

where $R_{TF} = \sqrt{2\mu_{TF}/m\omega_0^2}$ is the TF radius and $\mu_{TF} = \sqrt{2N}\hbar\omega_0$. When Eq. (10) is used in Eq. (2), the kinetic energy evaluates to

$$E_K[n_{TF}] = \frac{\sqrt{2}}{3}\hbar\omega_0 N^{3/2}, \quad (11)$$

which is the leading term in the large-N expansion of $E_{\rm ex}^K$. Thus, while Eq. (2) gives the quantum mechanical kinetic energy with the exact density as input, if the true variational density, Eq. (10), is used instead, the resulting kinetic energy is always *lower* than the exact kinetic energy. The upshot of all of this is that the TF energy functional, Eq. (3), will always produce a kinetic energy that is lower than the true value. This implies that the kinetic energy part of the TF functional has to be augmented by some correction in order to account for the second term in Eq. (9) [35].

We take the nonlocal correction to have the familiar von Weiszäcker (vW) form [23,36]

$$E_{\rm vW}[n] = \lambda_{\rm vW}(N)\frac{\hbar^2}{8m}\int d\mathbf{r}\frac{|\nabla n(\mathbf{r})|^2}{n(\mathbf{r})}, \quad (12)$$

where $\lambda_{\rm vW}(N)$ is a parameter which in general can depend on the particle number, N. This functional has the following desirable properties: (i) It depends on the gradient of the spatial density and thus vanishes in the limit of a uniform system; (ii) it is positive definite, thus increasing the kinetic energy relative to the TF approximation; (iii) it scales in the same way as $E_K[n]$ so that equipartition of kinetic and potential energy is preserved. The total energy functional for a noninteracting system in the TFvW approximation then reads [henceforth we suppress the N-dependence of $\lambda_{\rm vW}(N)$]

$$E[n] = \int d\mathbf{r}\left[\frac{\pi\hbar^2}{m}n(\mathbf{r})^2 + \lambda_{\rm vW}\frac{\hbar^2}{8m}\frac{|\nabla n(\mathbf{r})|^2}{n(\mathbf{r})} + v_{\rm ext}(\mathbf{r})n(\mathbf{r})\right]. \quad (13)$$

The variational minimization of this energy functional is conveniently achieved by introducing the so-called von Weiszäcker wave function $\psi(\mathbf{r}) \equiv \sqrt{n(\mathbf{r})}$. The Euler-Lagrange equation then takes the form of a nonlinear Schrödinger equation,

$$-\lambda_{\rm vW}\frac{\hbar^2}{2m}\nabla^2\psi(\mathbf{r}) + v_{\rm eff}(\mathbf{r})\psi(\mathbf{r}) = \mu\psi(\mathbf{r}), \quad (14)$$

where the effective potential is given by

$$v_{\rm eff}(\mathbf{r}) = \frac{2\pi\hbar^2}{m}\psi(\mathbf{r})^2 + v_{\rm ext}(\mathbf{r}). \quad (15)$$

Since $v_{\rm eff}(\mathbf{r})$ itself depends on $\psi(\mathbf{r})$, the solution of Eq. (14) must be determined self-consistently. The ground-state solution $\psi_0(\mathbf{r})$ with the normalization

$$\int d\mathbf{r}|\psi_0(\mathbf{r})|^2 = N, \quad (16)$$

determines the self-consistent ground-state density $n_0(\mathbf{r}) = \psi_0(\mathbf{r})^2$ and the chemical potential μ. We now establish that the vW correction can account for the exact energy of the harmonically confined system with a parameter $\lambda_{\rm vW}$ which is weakly N-dependent.

For a given number of particles N and a given value of $\lambda_{\rm vW}$, we determine $n_0(\mathbf{r})$ by solving the closed set of equations, viz., Eqs. (14) and (15), using the numerical method discussed in Sec. IV. This density is then used to evaluate $E[n_0]$ and the result is compared to $E_{\rm ex}$. The parameter $\lambda_{\rm vW}$ is then adjusted and the procedure is repeated until we achieve the equality

$$E[n_0] = E_{\rm ex}. \quad (17)$$

The net result of this procedure leads to the values of $\lambda_{\rm vW}$ plotted as a function of N in Fig. 1. The N-dependence is indeed weak and suggests that $\lambda_{\rm vW} \simeq 0.02$–$0.04$ for N in the range 10^2–10^6. These values of $\lambda_{\rm vW}$ are considerably smaller than the value ($\sim$0.25) found to be appropriate in 3D [37]. The inset to Fig. 1 illustrates the extrapolation to $N \to \infty$ and demonstrates that $\lambda_{\rm vW}$ has a nonzero limiting value.

To see in more detail how the vW energy accounts for the higher order terms in Eq. (9), it is convenient to expand $E[n_0]$

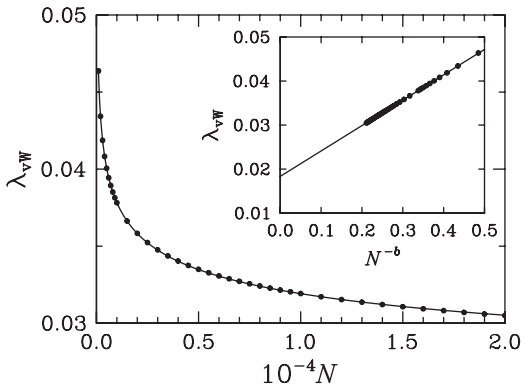

FIG. 1. The von Weiszäcker parameter $\lambda_{\rm vW}$ vs the number of particles N. The points are the calculated values and the smooth curve is the fit $\lambda_{\rm vW} = \lambda_{\rm vW}^{\infty} + a/N^b$ with $\lambda_{\rm vW}^{\infty} = 0.0184$, $a = 0.0577$, and $b = 0.1572$. The inset illustrates the extrapolation $N \to \infty$.

in terms of the difference $\Delta n \equiv n_0 - n_{TF}$. We have

$$E[n_0] = E_{TF}[n_0] + E_{\rm vW}[n_0] = E_{TF}[n_{TF}] + \frac{1}{2}m\omega_0^2 \int_{r\geqslant R_{TF}} d\mathbf{r}\big(r^2 - R_{TF}^2\big)\Delta n(\mathbf{r}) + \frac{\pi\hbar^2}{m}\int d\mathbf{r}[\Delta n(\mathbf{r})]^2 + E_{\rm vW}[n_0]. \quad (18)$$

Equating (18) to the large-N expansion of Eq. (8) and using $E_{TF}[n_{TF}] = (2\sqrt{2}/3)\hbar\omega_0 N^{3/2}$, we obtain

$$\frac{1}{12\sqrt{2}}\hbar\omega_0 N^{1/2} \simeq E_{\rm vW}[n_0] + \frac{1}{2}m\omega_0^2 \int_{r\geqslant R_{TF}} d\mathbf{r}\big(r^2 - R_{TF}^2\big)n_0(\mathbf{r}) + \frac{\pi\hbar^2}{m}\int d\mathbf{r}[n_0(\mathbf{r}) - n_{TF}(\mathbf{r})]^2. \quad (19)$$

Each of the integrals on the right-hand side, including the one defining $E_{\rm vW}[n_0]$, have integrands that peak near $r \sim R_{TF}$. Thus, the $N^{1/2}$ term in Eq. (9), which is a correction to the TF kinetic energy, can be interpreted as an edge correction. Since the last two terms on the right-hand side of Eq. (19) are small in comparison to $E_{\rm vW}[n_0]$, an approximate relation determining $\lambda_{\rm vW}$ would be

$$E_{\rm vW}[n_0] = \lambda_{\rm vW}\frac{\hbar^2}{8m}\int d\mathbf{r}\frac{|\nabla n_0|^2}{n_0} \simeq \frac{1}{12\sqrt{2}}\hbar\omega_0 N^{1/2}. \quad (20)$$

In applying this relation we again note that n_0 in Eq. (20) is an implicit function of $\lambda_{\rm vW}$. Thus, the procedure described earlier is followed and $\lambda_{\rm vW}$ is adjusted until $E_{\rm vW}[n_0]$ is equal to the right-hand-side of Eq. (20). This yields values of $\lambda_{\rm vW}$ which are about 10% larger than those obtained directly from Eq. (17).

To the extent that $\lambda_{\rm vW}$ is weakly N-dependent, Eq. (20) indicates that the integral $\int d\mathbf{r}|\nabla n_0|^2/n_0$ also scales roughly as $N^{1/2}$. This N-dependence is also exhibited by the integral with n_0 replaced with $n_{\rm ex}$, which is an indication that these densities are rather similar. In Fig. 2 we plot the self-consistent (solid line) and TFvW (dashed line) densities for different particle numbers. Even for the relatively small value of $N = 231$, these densities are in very good agreement and in fact are very close to n_{TF}, except at the edge of the cloud. The differences between

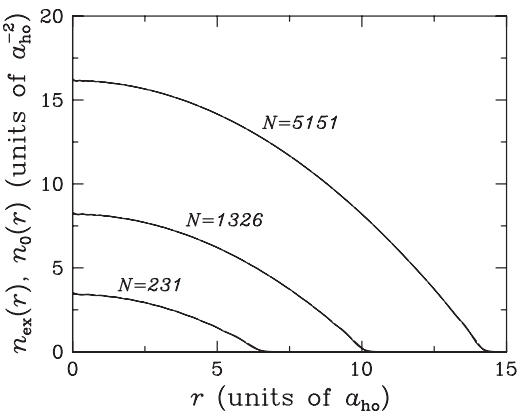

FIG. 2. The exact ($n_{\rm ex}$, solid line) and self-consistent (n_0, dashed line) densities as a function of the radial distance r for different numbers of particles N. Even for small particle numbers, the exact and TFvW densities are in very good agreement.

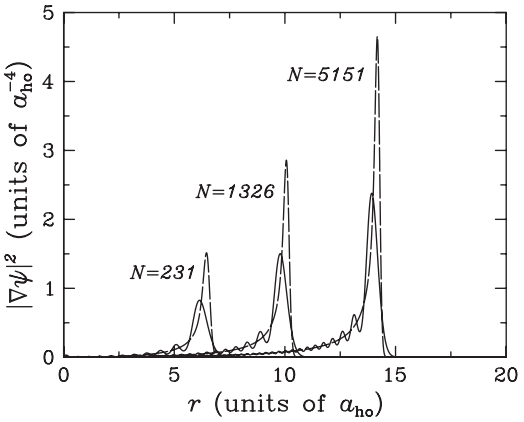

FIG. 3. The quantity $|\nabla\psi|^2 = \frac{1}{4}|\nabla n|^2/n$ contributing to the von Weiszäcker kinetic energy density in Eq. (12), evaluated using the exact (solid line) and self-consistent (dashed line) spatial densities as a function of the radial distance r for different numbers of particles N.

n_0 and $n_{\rm ex}$ are more clearly revealed by plotting $\frac{1}{4}|\nabla n|^2/n = |\nabla\psi|^2$ in Fig. 3. The integrals of the curves shown in Fig. 3 typically differ by about 15%. We note that the curves for the exact density (solid lines) exhibit prominent oscillations which are associated with the orbital shell structure. The fact that the TFvW curves (dashed lines) do not exhibit this shell structure is entirely expected in view of the semiclassical nature of the TFvW approximation [23]. However, we observe that the TFvW curves provide a smooth average of the shell oscillations (a well-known feature of semiclassical theories [23]) up to the edge of the cloud. At the edge, the TFvW approximation overestimates the exact value. In principle, this discrepancy can be reduced by including higher order gradient corrections to the kinetic energy functional, but for our purposes, this refinement is not necessary.

We summarize this section by noting that our analysis has shown that the corrections to the 2D LDA kinetic energy functional can indeed be represented in the gradient vW form, in spite of the fact that gradient expansion methods fail to produce any such terms in 2D. By comparing the results of the TFvW energy functional to the exact results for a harmonically confined noninteracting 2D gas, we are able to determine the vW parameter $\lambda_{\rm vW}$ and show that it is weakly N-dependent. We cannot claim that these values of $\lambda_{\rm vW}$ are generally applicable for problems in 2D but we would expect them to be appropriate for densities which are similar to those of the harmonically confined system. In particular, we expect the vW functional to be applicable for a harmonically confined system in which interactions are also included, as discussed in the following section.

III. DIPOLAR INTERACTIONS: HARTREE-FOCK APPROXIMATION

Having developed the approximate kinetic energy functional in the previous section, we are now in a position to construct the energy functional which accounts for the dipolar interactions in a 2D spin-polarized Fermi gas. The approach we adopt is essentially the one used for the analogous

problem with Coulomb interactions in 2D degenerate electronic systems. However, as we shall see, dipolar interactions lead to a fundamentally different energy functional. At the level of the Hartree-Fock (HF) approximation [20], the energy of the spin-polarized Fermi gas is $E_{HF} = E_K + E_{dd}$, where $E_K = \sum_{\mathbf{k}} n_{\mathbf{k}} \hbar^2 k^2/2m$ is the noninteracting kinetic energy and the dipole interaction energy is

$$E_{dd} = \frac{1}{2}\sum_{\mathbf{k}\mathbf{k}'} n_{\mathbf{k}} n_{\mathbf{k}'} [\langle \mathbf{k}\mathbf{k}'|V_{dd}|\mathbf{k}\mathbf{k}'\rangle - \langle \mathbf{k}\mathbf{k}'|V_{dd}|\mathbf{k}'\mathbf{k}\rangle]. \quad (21)$$

The first matrix element in Eq. (21) is the direct term and the second is the exchange term. For the singular dipolar interaction of interest (i.e., with the spins polarized perpendicular to the plane),

$$V_{dd}(r) = \frac{\mu_0 \mu^2}{4\pi r^3}, \quad (22)$$

each of these matrix elements are separately infinite. However, the sum of the two terms is finite as a result of the Pauli exclusion principle. This is seen most readily by writing the interaction energy as

$$E_{dd} = \frac{A}{2}\int d^2 r\, V_{dd}(\mathbf{r}) \bar{n}_{2D}^2 g_{HF}(\mathbf{r}), \quad (23)$$

where the HF radial distribution function is defined as

$$\bar{n}_{2D}^2 g_{HF}(\mathbf{r}) = \bar{n}_{2D}^2 - \left|\frac{1}{A}\sum_{\mathbf{k}} e^{-i\mathbf{k}\cdot\mathbf{r}}\right|^2. \quad (24)$$

Evaluating Eq. (24), we find

$$g_{HF}(\mathbf{r}) = 1 - \left(\frac{2J_1(k_F r)}{k_F r}\right)^2, \quad (25)$$

where $J_1(x)$ is the cylindrical Bessel function of order one [34]. The function $g_{HF}(r) - 1$ has a range of approximately k_F^{-1} and defines the "exchange hole" commonly used in electron-gas theory. For small r, $g_{HF}(r) \sim \frac{1}{4}(k_F r)^2$, and as a result, the integral in Eq. (23) is well behaved. We find

$$E_{dd} = \frac{1}{4} A \mu_0 \mu^2 \bar{n}_{2D}^2 k_F \int_0^\infty dt \frac{1}{t^2}\left[1 - \left(\frac{2J_1(t)}{t^2}\right)^2\right] = A\frac{64}{45\sqrt{\pi}}\mu_0 \mu^2 \bar{n}_{2D}^{5/2}. \quad (26)$$

Equation (26) has also been derived in the paper by Bruun and Taylor [2], and the final form is given by Fang and Englert [17]. In particular, Eq. (26) suggests that one can define an interaction energy functional within a LDA having the following form:

$$E_{dd}^{\mathrm{LDA}}[n] = \int d^2 r \frac{2}{5} C_{dd}[n(\mathbf{r})]^{5/2}, \quad (27)$$

with $C_{dd} \equiv (32/9\sqrt{\pi})\mu_0 \mu^2$. In contrast to the Coulomb problem, this local functional presumably accounts for the *total* interaction energy. To see if this is indeed reasonable, one must investigate in more detail the effect of density inhomogeneities.

Before doing so, we first provide an alternative derivation of Eq. (26), which assumes that $V_{dd}(r)$ has a well-defined Fourier transform (FT). This is achieved by defining a *regularized* dipole interaction $V_{dd}^{\mathrm{reg}}(r)$ which does not have the $r = 0$ singularity of $V_{dd}(r)$. As we shall see, a regularized interaction facilitates the corresponding analysis for an inhomogeneous system. Accepting for the moment that such an interaction is available, Eq. (21) becomes

$$E_{dd}^{\mathrm{reg}} = \frac{A}{2}\int \frac{d^2 k}{(2\pi)^2}\int \frac{d^2 k'}{(2\pi)^2}\theta(k_F - k)\theta(k_F - k') \times \left[\tilde{V}_{dd}^{\mathrm{reg}}(0) - \tilde{V}_{dd}^{\mathrm{reg}}(\mathbf{k} - \mathbf{k}')\right], \quad (28)$$

where $\tilde{V}_{dd}^{\mathrm{reg}}(\mathbf{k})$ is the 2D FT of $V_{dd}^{\mathrm{reg}}(r)$. With the change of variable $\mathbf{k}' = \mathbf{k} - \mathbf{q}$, Eq. (28) can be written as

$$E_{dd}^{\mathrm{reg}} = \frac{A}{2}\int \frac{d^2 q}{(2\pi)^4}\left[\tilde{V}_{dd}^{\mathrm{reg}}(0) - \tilde{V}_{dd}^{\mathrm{reg}}(\mathbf{q})\right] \times \int d^2 k\, \theta(k_F - k)\theta(k_F - |\mathbf{k} + \mathbf{q}|). \quad (29)$$

The second integral is just the area of overlap in momentum space of two circles of radius k_F whose centers are separated by q. This area is given by

$$A(q, k_F) = 2k_F^2\left[\cos^{-1}\left(\frac{q}{2k_F}\right) - \frac{q}{2k_F}\sqrt{1 - \left(\frac{q}{2k_F}\right)^2}\right] \times \theta(2k_F - q). \quad (30)$$

Substituting this result into Eq. (29), we find

$$E_{dd}^{\mathrm{reg}} = \frac{A k_F^4}{2\pi^3}\int_0^1 dx\, x[\cos^{-1} x - x\sqrt{1 - x^2}] \times \left[\tilde{V}_{dd}^{\mathrm{reg}}(0) - \tilde{V}_{dd}^{\mathrm{reg}}(2k_F x)\right]. \quad (31)$$

We now show that this expression reduces to Eq. (26) using an appropriate limiting procedure.

To this end, we now specify the regularized dipole interaction. This is done by considering the interaction between two physical *electric* dipoles [38], each of which has a charge distribution of the form

$$\rho(\mathbf{r}) = \frac{2\mathbf{p}\cdot\mathbf{r}}{\pi^{3/2}\sigma^5} e^{-r^2/\sigma^2}. \quad (32)$$

The electrostatic interaction between two dipoles $\mathbf{p}_1$ and $\mathbf{p}_2$ separated by $\mathbf{r}$ is

$$U(\mathbf{r}) = \frac{1}{\epsilon_0}\int \frac{d^3 k}{(2\pi)^3} e^{i\mathbf{k}\cdot\mathbf{r}} \frac{(\mathbf{p}_1\cdot\mathbf{k})(\mathbf{p}_2\cdot\mathbf{k})e^{-k^2\sigma^2/2}}{k^2} = -\frac{(\mathbf{p}_1\cdot\nabla)(\mathbf{p}_2\cdot\nabla)}{4\pi\epsilon_0}\left[\frac{1}{r}\mathrm{erf}\left(\frac{r}{\sqrt{2}\sigma}\right)\right], \quad (33)$$

where $\mathrm{erf}(x)$ is the error function. For $r \gg \sigma$, this interaction reduces to that of two *point* dipoles, varying as r^{-3}. However, for $r \ll \sigma$, the interaction saturates at a constant value as a result of the overlap of the dipole charge distributions.

Equation (33) can now be used to define a regularized *magnetic* dipole interaction for the spin-polarized Fermi gas by choosing $\mathbf{p}_1 = \mathbf{p}_2 = p\hat{\mathbf{z}}$, putting $\mathbf{r} = (x, y, 0)$ in Eq. (33), and replacing p^2/ϵ_0 with $\mu_0 \mu^2$. The regularized magnetic dipole

interaction then reads

$$V_{dd}^{\rm reg}(x,y) = \mu_0\mu^2 \int \frac{d^3k}{(2\pi)^3} e^{i(k_x x + k_y y)} \frac{k_z^2}{k^2} e^{-k^2\sigma^2/2} = \frac{\mu_0\mu^2}{4\pi}\left[\frac{1}{r^3}\mathrm{erf}\left(\frac{r}{\sqrt{2}\sigma}\right) - \sqrt{\frac{2}{\pi}}\frac{1}{\sigma r^2} e^{-r^2/2\sigma^2}\right]. \tag{34}$$

Equation (34) approaches Eq. (22) for $r \gg \sigma$ and saturates at $\mu_0\mu^2/3(2\pi)^{3/2}\sigma^3$ for $r \to 0$. The 2D FT of $V_{dd}^{\rm reg}(x,y)$ is

$$\tilde{V}_{dd}^{\rm reg}(q) = \mu_0\mu^2 e^{-q^2\sigma^2/2} \int \frac{dk_z}{2\pi} \frac{k_z^2}{k_z^2+q^2} e^{-k_z^2\sigma^2/2} = \frac{\mu_0\mu^2}{\sqrt{2\pi}\sigma}\left[e^{-q^2\sigma^2/2} - \sqrt{\frac{\pi}{2}} q\sigma\, \mathrm{erfc}\left(\frac{q\sigma}{\sqrt{2}}\right)\right]. \tag{35}$$

For $\sigma k_F \ll 1$, we see that

$$\tilde{V}_{dd}^{\rm reg}(0) - \tilde{V}_{dd}^{\rm reg}(2k_F x) \simeq \mu_0\mu^2 k_F x \tag{36}$$

to leading order in σk_F. Inserting this result into Eq. (31) we obtain

$$\lim_{\sigma\to 0} E_{dd}^{\rm reg} = A\frac{2\mu_0\mu^2 k_F^5}{45\pi^3}, \tag{37}$$

which is identical to Eq. (26). We thus see that the dipolar interaction energy can be obtained by taking the $\sigma \to 0$ limit in a calculation using an appropriately defined regularized dipole interaction. Of course the definition of the regularized potential is not unique, but the form we have chosen has particularly convenient properties. The essential reason for being able to use this approach is that the final result is insensitive to the cutoff σ when it becomes much smaller than the range k_F^{-1} of the exchange hole. This calculation can be viewed as the momentum-space version of the real space approach leading to Eq. (23).

We next proceed to a calculation of E_{dd} for an arbitrary *inhomogeneous* system making use of the regularized dipole interaction defined above. As we shall see, our real-space formulation leads to a final result that is identical to that obtained by Fang and Englert [17] using a Wigner function representation. However, our complementary derivation provides some additional insight into the interaction energy functional of the dipolar Fermi gas.

The generalization of Eq. (23) to an inhomogeneous spin-polarized system is

$$E_{dd} = \frac{1}{2}\int d^2r \int d^2r' [\rho(\mathbf{r},\mathbf{r})\rho(\mathbf{r}',\mathbf{r}') - \rho(\mathbf{r},\mathbf{r}')\rho(\mathbf{r}',\mathbf{r})] \times V_{dd}(\mathbf{r}-\mathbf{r}'), \tag{38}$$

where we have introduced the single-particle density matrix defined as

$$\rho(\mathbf{r},\mathbf{r}') = \sum_{i,\rm occ} \phi_i^*(\mathbf{r})\phi_i(\mathbf{r}'). \tag{39}$$

Here, the $\phi_i(\mathbf{r})$ are a set of single-particle states that correspond to a physical situation in which the density $n(\mathbf{r}) = \rho(\mathbf{r},\mathbf{r})$ is localized in space. The density matrix has the symmetry property $\rho(\mathbf{r},\mathbf{r}') = \rho(\mathbf{r}',\mathbf{r})$. The expression for E_{dd} in Eq. (38) is well-defined even for the singular dipole interaction; however, it is more difficult to exhibit the explicit cancellation between the direct and exchange terms for an inhomogeneous system. To achieve this cancellation we make use of the regularized interaction in Eq. (34) which allows us to evaluate the the direct and exchange terms separately. The desired result is then obtained by taking the $\sigma \to 0$ limit at the end of the calculation. As we show, the singular parts of the direct and exchange terms do, in fact, cancel exactly.

The direct term is calculated most conveniently in momentum space. We have

$$E_{dd}^{\rm (d)} = \frac{1}{2}\int \frac{d^2q}{(2\pi)^2} \tilde{V}_{dd}^{\rm reg}(q)|\tilde{n}(q)|^2. \tag{40}$$

To evaluate the exchange term, we introduce the center-of-mass variable $\mathbf{R} = (\mathbf{r}+\mathbf{r}')/2$ and the relative variable $\mathbf{s} = \mathbf{r}-\mathbf{r}'$. The exchange term can then be written as

$$E_{dd}^{\rm (x)} = -\frac{1}{2}\int d^2s\, V_{dd}^{\rm reg}(s) \int d^2R [\bar{\rho}(\mathbf{R},\mathbf{s})]^2, \tag{41}$$

where

$$\bar{\rho}(\mathbf{R},\mathbf{s}) \equiv \rho\big(\mathbf{R}+\tfrac{1}{2}\mathbf{s},\mathbf{R}-\tfrac{1}{2}\mathbf{s}\big). \tag{42}$$

The symmetry property of $\rho(\mathbf{r},\mathbf{r}')$ implies that $\bar{\rho}(\mathbf{R},-\mathbf{s}) = \bar{\rho}(\mathbf{R},\mathbf{s})$. We now define the function

$$f(\mathbf{s}) = \int d^2R [\bar{\rho}(\mathbf{R},\mathbf{s})]^2, \tag{43}$$

which satisfies $f(-\mathbf{s}) = f(\mathbf{s})$, and write

$$E_{dd}^{\rm (x)} = -\frac{1}{2}\int d^2s\, V_{dd}^{\rm reg}(s) f(\mathbf{s}) = -\frac{1}{2}\int d^2s V_{dd}^{\rm reg}(s)[f(\mathbf{s}) - f(0)] - \frac{1}{2}\int d^2s\, V_{dd}^{\rm reg}(s) f(0). \tag{44}$$

From Eq. (43) we have

$$f(0) = \int d^2R [n(\mathbf{R})]^2 = \int \frac{d^2q}{(2\pi)^2}|\tilde{n}(\mathbf{q})|^2, \tag{45}$$

where the last equality follows from Parseval's theorem, and we have noted that $n(\mathbf{R}) \equiv \bar{\rho}(\mathbf{R},0) = \rho(\mathbf{R},\mathbf{R})$. Combining Eqs. (40) and (44), we obtain

$$E_{dd} = \frac{1}{2}\int \frac{d^2q}{(2\pi)^2}\big[\tilde{V}_{dd}^{\rm reg}(q) - \tilde{V}_{dd}^{\rm reg}(0)\big]|\tilde{n}(\mathbf{q})|^2 - \frac{1}{2}\int d^2s\, V_{dd}^{\rm reg}(s)[f(\mathbf{s}) - f(0)]. \tag{46}$$

It should be emphasized that this result is valid for any potential $V_{dd}^{\rm reg}(r)$ which has a well-defined FT in the $q \to 0$ limit. In case the potential does not have a well-defined $q \to 0$ FT, one must revert to the expressions in Eqs. (40) and (41).

Making use of Eq. (35) and taking the $\sigma \to 0$ limit, we obtain

$$E_{dd} = -\frac{\mu_0\mu^2}{4}\int \frac{d^2q}{(2\pi)^2} q\,|\tilde{n}(\mathbf{q})|^2 + \frac{\mu_0\mu^2}{8\pi}\int d^2s\,\frac{1}{s^3}[f(0) - f(\mathbf{s})] \equiv E_{dd}^{(2)} + E_{dd}^{(1)}. \tag{47}$$

It can be shown that Eq. (47) is identical to the result obtained by Fang and Englert [17] and for this reason we have adopted their notation for the two terms. The term $E_{dd}^{(2)}$ appears explicitly in their paper but their $E_{dd}^{(1)}$ is given in a different form, being expressed in terms of the Wigner distribution function.

The $E_{dd}^{(1)}$ term involves the quantity

$$f(0) - f(\mathbf{s}) = \int d^2R\{[\bar{\rho}(\mathbf{R},0]^2 - [\bar{\rho}(\mathbf{R},\mathbf{s}]^2\} \equiv \int d^2R[n(\mathbf{R})]^2 g(\mathbf{s},\mathbf{R}). \tag{48}$$

Here we have defined the radial distribution function for the inhomogeneous system as

$$g(\mathbf{s},\mathbf{R}) = 1 - \frac{[\bar{\rho}(\mathbf{R},\mathbf{s})]^2}{[\bar{\rho}(\mathbf{R},0)]^2}. \tag{49}$$

An approximation to $E_{dd}^{(1)}$ can be generated by making a local approximation for $g(\mathbf{s},\mathbf{R})$, namely,

$$g(\mathbf{s},\mathbf{R}) \simeq g_{HF}(s; n(\mathbf{R})), \tag{50}$$

where the radial distribution function of the uniform gas is evaluated for a density equal to $n(\mathbf{R})$. With this replacement, we have

$$E_{dd}^{(1)} \simeq E_{dd}^{\mathrm{LDA}}, \tag{51}$$

as defined in Eq. (27). The total interaction includes the manifestly nonlocal $E_{dd}^{(2)}$ term.

We can check the validity of the LDA by evaluating Eq. (47) for a model inhomogeneous system. Specifically, we once again appeal to the ideal 2D Fermi gas confined by an isotropic harmonic trapping potential. This model is especially useful since the density matrix can be obtained in closed form for an arbitrary number of filled shells. Scaling all lengths by the harmonic oscillator length, a_{ho}, the one-particle density matrix for $M+1$ filled shells is given by [22]

$$\bar{\rho}(\mathbf{R},\mathbf{s}) = \frac{1}{\pi}\sum_{n=0}^{M}(-1)^n L_n(2R^2)e^{-R^2}L_{M-n}^1(s^2/2)e^{-s^2/4}, \tag{52}$$

where $L_n^\alpha(x)$ is the associated Laguerre polynomial [34]. We observe that for this particular model system, $\bar{\rho}(\mathbf{R},\mathbf{s})$ depends only on the magnitudes of the vectors $\mathbf{R}$ and $\mathbf{s}$, which is also true of all quantities derived from it. Putting $s=0$ in Eq. (52) yields the density $n(R)$ given by Eq. (6). (For convenience we drop the "ex" subscript in the following.) The FT of $n(R)$ is readily found to be given by

$$n(q) = L_M^2(q^2/2)e^{-q^2/4}. \tag{53}$$

We may also provide an explicit expression for the function $f(\mathbf{s})$, namely,

$$f(s) \equiv \int d^2R|\bar{\rho}(\mathbf{R},\mathbf{s})|^2 = \frac{1}{2\pi}\sum_{n=0}^{M}\left[L_n^1(s^2/2)\right]^2 e^{-s^2/2}. \tag{54}$$

Since all of the functions required for the evaluation of Eq. (47) depend only on the magnitude of the coordinates, the angular integrations can be performed immediately, leading to

$$\begin{aligned} E_{dd} &= -\frac{\mu_0\mu^2}{8\pi a_{\mathrm{ho}}^3}\int_0^\infty dqq^2|\tilde{n}(q)|^2 + \frac{\mu_0\mu^2}{4a_{\mathrm{ho}}^3}\int_0^\infty \frac{ds}{s^2}[f(0)-f(s)] \\ &= -\frac{\mu_0\mu^2}{8\pi a_{\mathrm{ho}}^3}\int_0^\infty dqq^2|\tilde{n}(q)|^2 - \frac{\mu_0\mu^2}{4a_{\mathrm{ho}}^3}\int_0^\infty \frac{ds}{s}\frac{df(s)}{ds}. \end{aligned} \tag{55}$$

Using Eq. (54) along with Eq. (53), we obtain

$$E_{dd}^{(1)} = \frac{\mu_0\mu^2}{8\pi a_{\mathrm{ho}}^3}\sum_{n=0}^{M}\left[\int_0^\infty ds 2L_{n-1}^2(s^2/2)L_n^1(s^2/2)e^{-s^2/2} + \int_0^\infty ds\left[L_n^1(s^2/2)\right]^2 e^{-s^2/2}\right]. \tag{56}$$

$$E_{dd}^{(2)} = -\frac{\mu_0\mu^2}{8\pi a_{\mathrm{ho}}^3}\int_0^\infty dqq^2\left[L_M^2(q^2/2)\right]^2 e^{-q^2/2}. \tag{57}$$

The function $L_{-1}^2(x)$, arising from the $n=0$ term in the summation of Eq. (56), should be interpreted as zero. All of the integrals in Eqs. (56) and (57) can be evaluated analytically, using the following general result [22]:

$$\begin{aligned} I_{mn}(\alpha,\beta,\gamma) &= \int_0^\infty dx x^\alpha e^{-x}L_m^\beta(x)L_n^\gamma(x) \\ &= \frac{\Gamma(1+\alpha)\Gamma(n+\gamma+1)\Gamma(\beta-\alpha+m)}{\Gamma(m+1)\Gamma(n+1)\Gamma(1+\gamma)\Gamma(\beta-\alpha)}\,{}_3F_2\left(1+\alpha-\beta,-n,1+\alpha;1+\gamma,1+\alpha-\beta-m;1\right), \end{aligned} \tag{58}$$

where ${}_3F_2(a,b,c;d,e;z)$ is the generalized hypergeometric function [34]. A direct application of Eq. (58) gives

$$E_{dd}^{(1)} = \frac{\mu_0\mu^2}{4\pi a_{\mathrm{ho}}^3}\frac{1}{\sqrt{2}}\sum_{n=0}^{M}\frac{(n+1)\Gamma(n+3/2)}{\Gamma(n+1)}\left\{\frac{4}{3}n\,{}_3F_2\left(-\frac{3}{2},\frac{1}{2},-n;2,-\frac{1}{2}-n;1\right) + {}_3F_2\left(-\frac{1}{2},\frac{1}{2},-n;2,-\frac{1}{2}-n;1\right)\right\}, \tag{59}$$

$$E_{dd}^{(2)} = -\frac{\mu_0\mu^2}{4\pi a_{\mathrm{ho}}^3}\frac{1}{2\sqrt{2}}\frac{\Gamma\left(M+\frac{3}{2}\right)(M+1)(M+2)}{\Gamma(M+1)}\,{}_3F_2\left(\frac{1}{2},\frac{3}{2},-M;2,\frac{1}{2}-M;1\right). \tag{60}$$

TABLE I. Comparison of the dipolar interaction energies with the LDA. The last column corresponds to the relative percentage error between the exact total energy, $E_{dd}^{\rm exact} = E_{dd}^{(1)} + E_{dd}^{(2)}$, and $E_{dd}^{\rm LDA}$. The unit of energy is $\mu_0\mu^2/a_{\rm ho}^3$.

N	$E_{dd}^{(1)}$	$E_{dd}^{\rm LDA}$	$E_{dd}^{(2)}$	$\Delta E/E\%$
55	54.4003	54.5724	−6.8321	15
105	168.6535	168.9366	−15.3065	10
231	670.199	670.718	−40.9666	7
1326	14 266.3	14 268.3	−363.681	3
5151	153 345.6	153 349.4	−1983.06	1

While these final expressions are not particularly illuminating, they do provide summations which are easily dealt with numerically. On the other hand, the integrands in Eqs. (56) and (57) become highly oscillatory when the index n is large and the evaluation of the integrals can be problematic without the use of specialized numerical integration techniques.

In Table I we give values of $E_{dd}^{(1)}$, $E_{dd}^{(2)}$, and $E_{dd}^{\rm LDA}$ for a range of particle numbers, N. We see that $E_{dd}^{(1)} \simeq E_{dd}^{\rm LDA}$ to a very good approximation even for relatively small numbers of particles. To quantify this further we show in Fig. 4 a comparison of $g_{HF}(s;n(R))$ and $g(s,R)$ for $M = 20\,(N = 231)$ for R ranging from the center of the cloud to its edge. We see that the local approximation in Eq. (50) is very good; the local Fermi wave vector $k_F(R)$ captures very nicely the extent of the exchange hole in the exact radial distribution function. These observations explain why $E_{dd}^{(1)}$ is so close to $E_{dd}^{\rm LDA}$. Although these results have been obtained for the specific model of a harmonically confined gas, we would expect similar behavior whenever the model density varies on a length scale which is large compared to the extent of the local exchange hole.

Table I also shows that the nonlocal contribution diminishes rapidly with respect to the local contribution with increasing N. Indeed, it is straightforward to show that the $N \gg 1$ behaviors of the two contributions are $E_{dd}^{(1)} \sim N^{7/4}$ and $|E_{dd}^{(2)}| \sim N^{5/4}$. Therefore, we find that $|E_{dd}^{(2)}/E_{dd}^{(1)}| \sim 1/\sqrt{N}$ in the large-N limit. As a result, the *total* interaction energy is very well approximated by $E_{dd}^{\rm LDA}$ for large N, as illustrated in Table I.

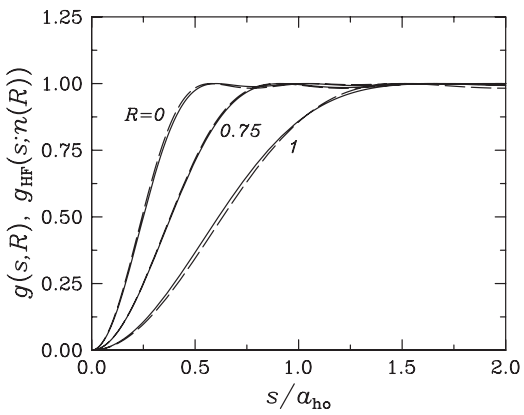

FIG. 4. Comparison of the exact radial distribution function (solid line) with the local approximation (dashed line). The values of R indicated are in units of the TF radius R_{TF}. The number of particles is $N = 231$ ($M = 20$).

This local energy functional for the total interaction energy can thus be trusted in applications, such as those typically encountered in traps, where the density of the system is a smooth and slowly varying function of position.

We wish to emphasize that the locality of the interaction energy functional is a property of the dipolar interaction and is not generally valid. To illustrate this we can compare these results with those obtained for an interparticle Coulomb interaction, $e^2/4\pi\epsilon_0 r$. There is no need to regularize the potential in this case and the direct and exchange terms can be evaluated directly from Eq. (38). For consistency we again consider a spin-polarized situation. The direct contribution is

$$E_{ee}^{(\rm d)} = \frac{e^2}{8\pi\epsilon_0}\int \frac{d^2q}{(2\pi)^2}\frac{2\pi}{q}|n(\mathbf{q})|^2, \tag{61}$$

where $2\pi/q$ is the 2D FT of r^{-1}. The exchange term reads

$$E_{ee}^{(\rm x)} = -\frac{e^2}{8\pi\epsilon_0}\int \frac{d^2s}{s} f(\mathbf{s}). \tag{62}$$

Using Eqs. (53) and (54) for the isotropic 2D harmonic trap, we find

$$E_{ee}^{(\rm d)} = \frac{e^2}{4\pi\epsilon_0 a_{\rm ho}}\frac{1}{3\sqrt{2}}\frac{\Gamma\left(M+\frac{5}{2}\right)\Gamma(M+3)}{\Gamma(M+1)^2} \times {}_3F_2\left(-\frac{3}{2},\frac{1}{2},-M;3,-\frac{3}{2}-M;1\right), \tag{63}$$

and

$$E_{ee}^{(\rm x)} = -\frac{e^2}{4\pi\epsilon_0 a_{\rm ho}}\frac{1}{\sqrt{2}}\sum_{n=0}^{M}\frac{\Gamma\left(n+\frac{3}{2}\right)(n+1)}{\Gamma(n+1)} \times {}_3F_2\left(-\frac{1}{2},\frac{1}{2},-n;2,-\frac{1}{2}-n;1\right). \tag{64}$$

The sum of these energies can be thought of as an approximation to the interaction energy of a 2D parabolic quantum dot. The 2D (spin-polarized) Dirac exchange functional in the LDA is given by

$$E_{ee}^{(\rm x),\rm LDA}[n] = -\frac{e^2}{4\pi\epsilon_0 a_{\rm ho}}\frac{8}{3\sqrt{\pi}}\int d^2r[n(r)]^{3/2}. \tag{65}$$

We compare the various energies in Table II. We see that the LDA is again a very good approximation to the exchange energy. The direct Coulomb energy is, of course, inherently nonlocal and is seen to give the dominant interaction energy contribution for large N, in contrast to the situation for the

TABLE II. Comparison of the Coulomb interaction energy with the exchange energy calculated exactly and in the LDA. The last column gives the relative percentage error between the exact exchange energy, Eq. (64), and the exchange energy obtained from the Dirac functional, Eq. (65). The energies are in units of $e^2/4\pi\epsilon_0 a_{\rm ho}$.

N	$E_{ee}^{(\rm x)}$	$E_{ee}^{(\rm x),\rm LDA}$	$E_{ee}^{(\rm d)}$	$\Delta E/E\%$
55	−85.8544	−85.4033	683.615	0.5
105	−192.347	−191.746	2119.36	0.3
231	−514.802	−513.958	8421.97	0.2
1326	−4570.15	−4568.39	179 276.2	0.04
5151	−24 919.8	−24 911.7	$1.926\,99 \times 10^6$	0.03

dipolar interaction where the local contribution dominates. In fact, it can readily be shown that $|E_{ee}^{(x)}/E_{ee}^{(d)}| \sim 1/\sqrt{N}$ for $N \gg 1$.

To summarize, we have shown that even for modest values of the particle number, N, the total interaction energy for the harmonically trapped, 2D dipolar Fermi gas can be approximately represented by a *local* energy functional. We must emphasize again that the locality of the density functional for the dipolar gas is a result of the short-range $\sim 1/r^3$ behavior of the dipole-dipole interaction, in contrast to e.g., the Coulomb interaction, in which case the *total* interaction energy cannot be reduced to a purely local form.

We now have all of the necessary components to construct the TFvW energy functional for a 2D, harmonically trapped interacting dipolar Fermi gas, viz.,

$$E[n] = \int d\mathbf{r} \left[\frac{1}{2} C_K n(\mathbf{r})^2 + \lambda_{\rm vW} \frac{\hbar^2}{8m} \frac{|\nabla n(\mathbf{r})|^2}{n(\mathbf{r})} + \frac{2}{5} C_{dd} [n(\mathbf{r})]^{5/2} + v_{\rm ext}(\mathbf{r}) n(\mathbf{r}) \right], \tag{66}$$

where $C_K = 2\pi\hbar^2/m$. Once again, introducing the vW wave function and performing the variational minimization of Eq. (66) with respect to the density gives

$$-\lambda_{\rm vW} \frac{\hbar^2}{2m} \nabla^2 \psi(\mathbf{r}) + v_{\rm eff}(\mathbf{r}) \psi(\mathbf{r}) = \mu \psi(\mathbf{r}), \tag{67}$$

where now $v_{\rm eff}(\mathbf{r})$ also contains an interaction term, viz.,

$$v_{\rm eff}(\mathbf{r}) = C_K \psi(\mathbf{r})^2 + C_{dd} \psi(\mathbf{r})^3 + v_{\rm ext}(\mathbf{r}). \tag{68}$$

Along with the normalization condition, Eq. (16), Eq. (67) provides a complete description for the ground-state spatial density of the system.

IV. SELF-CONSISTENT EQUILIBRIUM SOLUTIONS

The numerical self-consistent solution of Eq. (67) was achieved by means of imaginary time propagation (ITP) [39]. In this method, the time-dependent Schrödinger equation

$$\frac{\partial \psi(\mathbf{r},\tau)}{\partial \tau} = -\frac{H(\tau)}{\hbar} \psi(\mathbf{r},\tau), \tag{69}$$

is evolved in imaginary time, $t \to -i\tau$, starting from some arbitrary initial state $\psi(\mathbf{r},0)$. The Hamiltonian governing the evolution is

$$H(\tau) = -\lambda_{\rm vW} \frac{\hbar^2 \nabla^2}{2m} + v_{\rm eff}(\mathbf{r},\tau) \equiv T + V(\tau), \tag{70}$$

where the time dependence arises from the dependence of $v_{\rm eff}$ on the evolving density $n(\mathbf{r},\tau) = \psi(\mathbf{r},\tau)^2$. The evolution is carried out in a stepwise fashion according to

$$\psi(\mathbf{r},\tau + \Delta\tau) = e^{-H(\tau)\Delta\tau/\hbar} \psi(\mathbf{r},\tau). \tag{71}$$

The repeated application of the evolution operator yields a wave function $\psi(\mathbf{r},\tau)$ which eventually converges to the self-consistent ground state $\psi_0(\mathbf{r})$ as $\tau \to \infty$.

The evolution in Eq. (71) is achieved by using the split-operator approximation [39,40]

$$e^{-H(\tau)\Delta\tau/\hbar} \simeq e^{-V(\tau)\Delta\tau/2\hbar} e^{-T\Delta\tau/\hbar} e^{-V(\tau)\Delta\tau/2\hbar}, \tag{72}$$

together with fast Fourier transforms (FFTs) [41] to convert between coordinate and momentum spaces. If a Cartesian grid is used in the x and y directions for our 2D geometry, 2D FFTs are required. However, a more efficient algorithm is available if the system possesses circular symmetry. The kinetic energy operator in this case takes the form

$$T = -\lambda_{\rm vW} \frac{\hbar^2}{2m} \frac{d^2}{dr^2} + \lambda_{\rm vW} \frac{\hbar^2}{2m} \frac{1}{r} \frac{d}{dr} \equiv T_1 + T_2. \tag{73}$$

With this decomposition, the evolution operator becomes

$$e^{-H(\tau)\Delta\tau/\hbar} \simeq e^{-V(\tau)\Delta\tau/2\hbar} e^{-T_2\Delta\tau/2\hbar} e^{-T_1\Delta\tau/\hbar} e^{-T_2\Delta\tau/2\hbar} \times e^{-V(\tau)\Delta\tau/2\hbar}, \tag{74}$$

where the T_1 step is again treated by means of FFTs, but now with respect to the 1D radial variable r in the range $[-R,R]$. The kinetic step T_2, on the other hand, is treated in coordinate space using a Crank-Nicholson method [41], which requires the solution of a tridiagonal system, viz.,

$$-\phi(r_{i+1}) + \alpha_i \phi(r_i) + \phi(r_{i-1}) = \bar{\phi}(r_{i+1}) + \alpha_i \bar{\phi}(r_i) - \bar{\phi}(r_{i-1}), \tag{75}$$

where $\alpha_i = \frac{4r_i}{\lambda_{\rm vW}} \frac{\Delta r}{\Delta \tau}$, and $\bar{\phi}(r_i)$ is the wave function prior to the application of the T_2 evolution operators. The solution to Eq. (75) is uniquely determined by Dirichlet boundary conditions at the ends of the r_i mesh, where the wave function is required to vanish. At the end of each time step we update H with the new $n(r,\tau)$ which is properly normalized to N. The convergence criterion for achieving self-consistency is taken to be $\sum_i |\psi(r_i,\tau_n) - \psi(r_i,\tau_{n-1})| < \varepsilon$, where typically $\varepsilon \lesssim 10^{-6}$. Once self-consistency has been achieved, the chemical potential is given by $\mu = \langle \psi_0 | H | \psi_0 \rangle$ and the ground-state energy is obtained from Eq. (66). This numerical procedure can also be adapted with minor modifications to spherically symmetric 3D systems.

In Fig. 5 we present the TFvW self-consistent ground-state density profile for $N = 100$ for various strengths of the dipole-dipole interaction. With increasing interaction strength, the radius of the atomic cloud increases and the central density decreases, which is expected given the repulsive nature of the

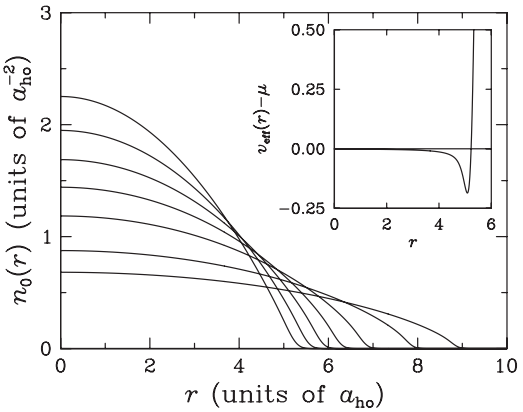

FIG. 5. Density distributions for $N = 100$. The curves with increasing radial extent correspond to $C_{dd}/C_K = 0$, 0.2, 0.5, 1.0, 2.0, 5.0, 10.0. The inset shows the effective potential in units of $\hbar\omega_0/2$, as a function of r in units of $a_{\rm ho}$, in the noninteracting limit, $C_{dd}/C_K = 0$.

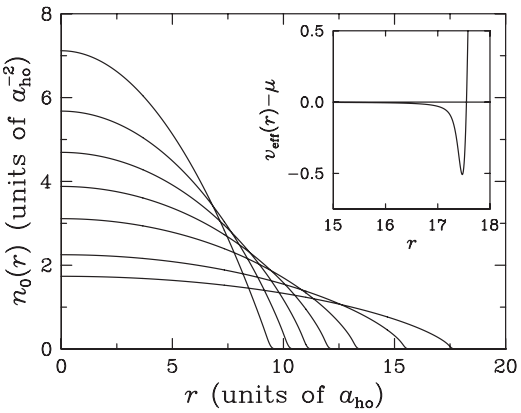

FIG. 6. Density distributions for $N = 1000$. The curves with increasing radial extent correspond to $C_{dd}/C_K = 0, 0.2, 0.5, 1.0, 2.0, 5.0, 10.0$. The inset shows the effective potential in units of $\hbar\omega_0/2$, as a function of r in units of a_{ho}, in the case of strong interactions, $C_{dd}/C_K = 10.0$.

dipole-dipole interaction for the spin-polarized case. As found for the $C_{dd} = 0$ case considered earlier, the vW gradient term has the effect of giving a density that decays smoothly in the classically forbidden region defined by $v_{eff}(r) > \mu$. We recall that if the vW term is absent, the spatial density has an unphysical sharp cutoff at a radius R defined by $v_{eff}(R) = \mu'$, where μ' is the chemical potential in this approximation. For $C_{dd}/C_K \gg 1$, $R \propto N^{3/10}$. In Fig. 6, we show the spatial density for $N = 1000$. It is apparent that the effect of the vW term becomes less significant as the number of particles is increased. This trend increases with increasing N and the density approaches the distribution found in the local density approximation. In the insets to Figs. 5 and 6 we have also included representative plots of the effective potential for the case $C_{dd}/C_K = 0$ in Fig. 5 and $C_{dd}/C_K = 10$ in Fig. 6. The potential is essentially flat up to the edge of the cloud where it falls below the chemical potential and then rises quadratically. The main point to be taken from these curves is that the shape of the effective potential is not very sensitive to the introduction of interactions. Finally, we note that our equilibrium density profiles are very similar to those found in Ref. [17] without the vW correction. The latter densities would be virtually indistinguishable from those plotted in Figs. 5 and 6 except in the classically forbidden region where the vW gradient correction leads to densities which decay smoothly to zero.

V. CONCLUSIONS

We have presented a mathematically simple and computationally efficient DFT formulation of the equilibrium properties of a 2D trapped dipolar Fermi gas based on the TFvW approximation. One of the key elements of this work is the development of a kinetic energy functional appropriate for an inhomogeneous 2D system. Specifically, we have shown that the addition of a vW-like gradient correction to the TF kinetic energy functional is needed in order to accurately determine the ground-state energy, as well as to provide a physically reasonable density distribution at the edge of the cloud. While conventional gradient expansions in 2D fail to yield gradient corrections to the TF kinetic energy functional, our detailed analysis has provided a compelling argument for the inclusion of a vW-like gradient correction. We have also provided an alternative derivation of the interaction energy functional first obtained by Fang and Englert [17]. We find in particular that the exchange hole is a useful concept in formulating the local density approximation and furthermore explains the underlying reasons behind the local nature of the total interaction functional.

We have also presented a highly efficient self-consistent numerical scheme for determining the equilibrium spatial density distributions within the TFvW formalism. Our calculations illustrate how the strength of the (repulsive) dipole-dipole interaction affects the size of the cloud and its spatial distribution. Although the vW gradient correction does not modify substantially the density in the interior of the cloud, it does yield a density which decays smoothly into the classically forbidden region at the edge. This feature is particularly important in performing calculations of the collective mode frequencies using TFvW hydrodynamics [10,16], and will be addressed in a future presentation. In addition, it will be of interest to investigate the affect of the anisotropy of the dipole-dipole interaction in a confined 2D system by considering the situation in which the spins are canted at some angle with respect to the 2D plane. Finally, although we have focused on the 2D geometry, we wish to emphasize that the extension of the TFvW theory to 3D is straightforward.

ACKNOWLEDGMENT

This work was supported by the Natural Sciences and Engineering Research Council of Canada (NSERC).

[1] For a recent review, see, e.g., M. Baranov, Phys. Rep. **464**, 71 (2008), and references therein.
[2] G. M. Bruun and E. Taylor, Phys. Rev. Lett. **101**, 245301 (2008).
[3] R. Chicireanu, A. Pouderous, R. Barbe, B. Laburthe-Tolra, E. Marechal, L. Vernac, J.-C. Keller, and O. Gorceix, Phys. Rev. A **73**, 053406 (2006).
[4] A. J. Berglund, S. A. Lee, and J. J. McClelland, Phys. Rev. A **76**, 053418 (2007).
[5] K. K. Ni, S. Ospelkaus, D. Wang, G. Quemener, B. Neyenhuis, M. H. G. de Miranda, J. L. Bohn, J. Ye, and D. S. Jin, Nature (London) **464**, 1324 (2010).
[6] A. Chotia, B. Neyenhuis, S. A. Moses, B. Yan, J. P. Covey, M. Foss-Feig, A. M. Rey, D. S. Jin, and J. Ye, Phys. Rev. Lett. **108**, 080405 (2012).
[7] M. Lu, N. Q. Burdick, and B. L. Lev, Phys. Rev. Lett. **108**, 215301 (2012).
[8] L. M. Sieberer and M. A. Baranov, Phys. Rev. A **84**, 063633 (2011).
[9] M. A. Baranov, L. Dobrek, and M. Lewenstein, Phys. Rev. Lett. **92**, 250403 (2004).
[10] E. Zaremba and H. C. Tso, Phys. Rev. B **49**, 8147 (1994).
[11] E. Zaremba, Phys. Rev. B **53**, R10512 (1996).

[12] B. P. van Zyl, Ph.D. thesis, Queen's University, 2000.
[13] M. Hochgräfe, B. P. van Zyl, Ch. Heyn, D. Heitmann, and E. Zaremba, Phys. Rev. B **63**, 033316 (2001).
[14] B. P. van Zyl and E. Zaremba, Phys. Rev. B **63**, 245317 (2001).
[15] B. P. van Zyl, E. Zaremba, and D. A. W. Hutchinson, Phys. Rev. B **61**, 2107 (2000).
[16] B. P. van Zyl and E. Zaremba, Phys. Rev. B **59**, 2079 (1999).
[17] B. Fang and B-G. Englert, Phys. Rev. A **83**, 052517 (2011).
[18] W. Kohn and L. J. Sham, Phys. Rev. **140**, A1133 (1965).
[19] P. Hohenberg and W. Kohn, Phys. Rev. **136**, B864 (1964).
[20] R. M. Dreizler and E. K. U. Gross, *Density Functional Theory: An Approach to the Quantum Many-Body Problem* (Springer-Verlag, Berlin, 1990).
[21] M. Brack and B. P. van Zyl, Phys. Rev. Lett. **86**, 1574 (2001).
[22] B. P. van Zyl, Phys. Rev. A **68**, 033601 (2003).
[23] M. Brack and R. K. Bhaduri, *Semiclassical Physics*, Frontiers in Physics Vol. 96 (Addison-Wesley, Reading, MA, 2003).
[24] D. A. Kirzhnits, Sov. Phys. JETP **5**, 64 (1957).
[25] W. Jones and W. H. Young, J. Phys. C: Solid State Phys. **4**, 1322 (1971).
[26] C. H. Hodges, Can. J. Phys. **51**, 1428 (1973).
[27] A. Holas, P. M. Koslowski, and N. H. March, J. Phys. A: Math. Gen. **24**, 4249 (1991).
[28] L. Salasnich, J. Phys. A: Math. Theor. **40**, 9987 (2007).
[29] M. Koivisto and M. J. Stott, Phys. Rev. B **76**, 195103 (2007).
[30] A. Putaja, E. Räsänen, R. van Leeuwen, J. G. Vilhena, and M. A. L. Marques, Phys. Rev. B **85**, 165101 (2012).
[31] N. Choudhury and S. K. Ghosh, Phys. Rev. B **51**, 2588 (1995).
[32] S. Stern, Phys. Rev. Lett. **18**, 546 (1967).
[33] In the Wigner-Kirkwood semiclassical approach, the kinetic energy density for the spin polarized system in 2D is found to be $\tau_0[n] = \frac{\hbar^2}{m}[\pi n^2 + \frac{1}{6}\nabla^2 n + \frac{1}{24}\delta(n)(\nabla n)^2]$ [12]. These gradient corrections, however, give a vanishing contribution to the integrated kinetic energy for physical densities which decay *smoothly* to zero as r tends to infinity. Thus, these corrections can be ignored within any density functional scheme which produces physically smooth densities.
[34] I. S. Gradshteyn and I. M. Ryzhik, *Table of Inegrals, Series, and Products*, 4th ed. (Academic Press, New York, 1980).
[35] If the TF density, Eq. (10), is used in the Wigner-Kirkwood (WK) kinetic energy functional [33], the resulting correction to the energy is identical in form to the second term in Eq. (9), but with a numerical coefficient which is too large. This correction arises from the *nonanalytic* behavior at the edge of the TF density. It can therefore be interpreted as an *edge* correction.
[36] C. F. von Weizsacker, Z. Phys. **96**, 431 (1935).
[37] A. Chizmeshya and E. Zaremba, Phys. Rev. B **37**, 2805 (1988).
[38] It should be emphasized that the consideration of *electric* dipoles is merely a convenient way of generating a regularized *magnetic* dipolar interaction to be used in 2D. Electric and magnetic dipolar interactions are, of course, not interchangable in 3D since they give rise to distinct contact interactions. Such contact interactions do not arise in 2D.
[39] H. F. Trotter, Proc. Am. Math. Soc. **10**, 545 (1959)
[40] G. Strang, SIAM J. Numer. Anal. **5**, 506 (1968).
[41] W. H. Press, S. A. Teukolsky, W. T. Vetterling, and B. P. Flannery, *Numerical Recipes: The Art of Scientific Computing*, 3rd ed. (Cambridge University Press, New York, 2007).